

## Surface phonon dispersion of platinum (111)

Klaus Kern, Rudolf David, Robert L. Palmer, and George Comsa  
*Institut für Grenzflächenforschung und Vakuumphysik, Kernforschungsanlage Jülich,  
 Postfach 1913, D-5170 Jülich, Germany*

Talat S. Rahman

*Cardwell Hall, Department of Physics, Kansas State University, Manhattan, Kansas 66506*  
 (Received 9 September 1985)

The dispersion of the vibrational modes of the Pt(111) surface has been measured by inelastic He scattering along the  $\bar{\Gamma}$ - $\bar{M}$  and  $\bar{\Gamma}$ - $\bar{K}$  azimuths of the two-dimensional Brillouin zone for the first time. Significant asymmetry between the two crystal directions is observed. A lattice-dynamical analysis gives good agreement with the data when the intralayer force constant of the Pt atoms in the first layer is reduced to 40% of its value in the bulk.

Surface phonon spectroscopy, which became feasible only in the last few years, has proved to be an excellent approach to understanding the structure and dynamics of surfaces. Information on surface geometry and the corresponding binding forces can now be obtained from the observed phonon dispersion. There are presently only two major techniques for the experimental investigations of surface phonons: inelastic scattering of He atoms<sup>1</sup> and inelastic scattering of low-energy electrons (electron-energy-loss spectroscopy).<sup>2</sup> Both methods have their pros and cons. Besides its obvious advantages—very high energy resolution and nondestructiveness—inelastic He scattering is primarily limited by the strong decrease of the cross section for phonon excitation with increasing phonon energy. Inelastic electron scattering is more constrained by its resolution than by intensity. The two methods appear to be complementary.<sup>2</sup>

The dispersion of the (111) surface phonons of several fcc metals (Cu, Ag, and Au) has recently been measured using He scattering.<sup>3,4</sup> Although the  $\langle 110 \rangle$  direction of the (111) surface of fcc crystals exhibits lower symmetry than the  $\langle 112 \rangle$  direction, none of these experiments indicates a significantly different dispersion behavior along these two symmetry directions. In particular, the Rayleigh modes are reported to be nearly identical for each of the three metals in these two directions. Here we report results for inelastic He scattering from a Pt(111) surface that reveal significant differences between the dispersion curves along the two directions. The measured surface phonon dispersions are compared with theoretical calculations based on a nearest-neighbor central-force model.<sup>5</sup> We find reasonable agreement between the data and the lattice-dynamical calculations.

The experimental setup consists of a nozzle beam source,<sup>6</sup> a target chamber, and a differentially pumped time-of-flight (TOF) spectrometer.<sup>7</sup> The measurements are performed at a fixed total scattering angle of 90°. The nozzle beam is produced by expanding helium through a 5- $\mu$ m-diam nozzle; the results shown here were obtained at nozzle pressures in the range 160–220 bars at several nozzle temperatures between 45–125 K, yielding average translational energies in the range 10–27 meV with a velocity spread  $\Delta v/v \leq 1\%$  (full width at half-maximum).<sup>7</sup> TOF analysis of the scattered helium beam is performed by means of pseudorandom chopping with 10- $\mu$ sec time resolu-

tion (flight path 790 mm). The effective energy resolution is between 0.3 and 0.6 meV. The TOF distribution is obtained by cross correlation carried out by means of an on-line computer.<sup>8</sup> The angular spread of the incident beam and the angle subtended by the ionizer opening are both equal to 0.2°, i.e., the full instrumental angular resolution is 0.3°. The Pt(111) crystal is mounted in an ultrahigh-vacuum chamber, with a base pressure of  $4 \times 10^{-11}$  Torr, on a manipulator that allows independent polar and azimuthal rotation and tilting. The target temperature can be regulated between 25 and 1800 K. The Pt(111) single crystal is cleaned by repeated cycles of argon-ion bombardment and annealing to 1200 K as well as by annealing in an oxygen atmosphere ( $\sim 5 \times 10^{-7}$  Torr) to 900 K until no traces of impurities can be detected by the cylindrical-mirror-analyzer Auger spectrometer. The defect density of the clean crystal is less than  $10^{-3}$  as probed with elastic He scattering.<sup>9</sup> The azimuthal alignment of the crystal is performed *in situ* by means of He diffraction. The  $\langle 112 \rangle$  azimuth is easily aligned by maximizing the  $(\bar{1}\bar{1})$  diffraction peak of the clean platinum surface. Because in the  $\langle 110 \rangle$  direction the Pt diffraction peak is substantially smaller, this azimuth is aligned by maximizing the  $(\bar{1}\bar{1})$  diffraction peak of the commensurate  $(\sqrt{3} \times \sqrt{3})R30^\circ$  Xe overlayer.<sup>10</sup>

Figure 1(a) shows a series of TOF spectra of clean Pt(111) taken along the  $\bar{\Gamma}$ - $\bar{K}$  azimuth. The arrows on the bottom mark the diffuse elastic peak, which is due to scattering at defects. The significant phonon events are marked by arrows above the peaks. Phonon momentum and energy are determined from the TOF peak and incident angle, using conservation of energy and momentum. Under the kinematic constraints imposed by the experimental conditions of Fig. 1 ( $E_i = 27$  meV,  $40^\circ > \theta_i > 29^\circ$ ) and in the absence of a strong diffraction peak on close-packed metal surfaces, only created phonons are observed.<sup>11</sup> At angles close to the specular, only one sharp phonon (Rayleigh) mode is detected. With decreasing incident angle the phonon peak broadens and, between 35° and 31°, a clear splitting is obvious. The peak splitting is only seen for low surface temperatures  $T_s < 200$  K and high surface quality. The relative height of the diffuse elastic peak is an excellent measure for the surface quality. In order to see the splitting, the diffuse elastic peak cannot be larger than the phonon peak at  $T_s = 25$  K and, correspondingly much smaller

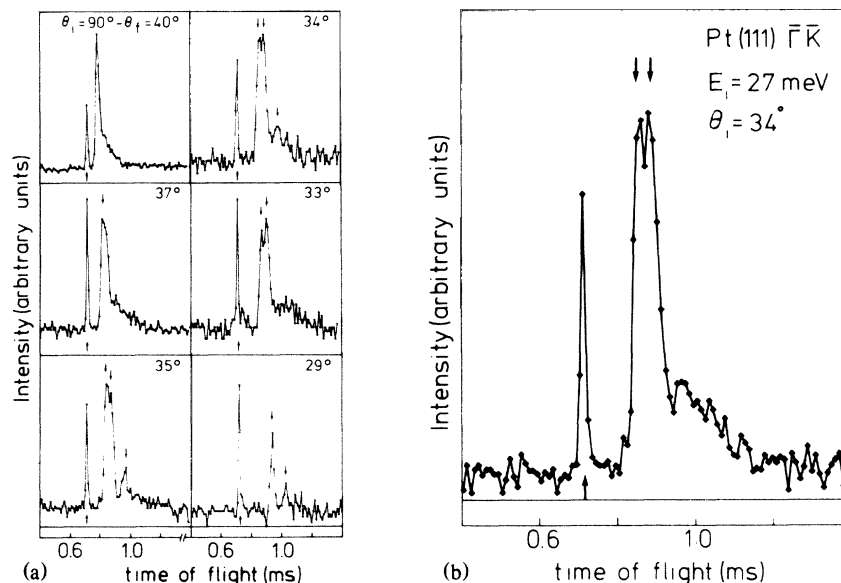


FIG. 1. (a) Series of TOF spectra for the  $\bar{\Gamma}$ - $\bar{K}$  azimuth at a crystal temperature of 25 K and a He-beam energy of 27 meV. With decreasing incident angle  $\theta_i$ , phonons with higher phonon momentum and energy are probed. (b) TOF spectrum at  $\theta_i = 34^\circ$  with improved signal to noise ratio, 3.5 h measuring time.

near 200 K. If the diffuse elastic peak is substantially larger, the phonon peak is unusually broad between  $35^\circ$  and  $31^\circ$ , but no splitting can be seen. Each spectrum was recorded immediately after flashing and rapidly cooling the crystal. The recording time per spectrum in Fig. 1(a) was 30 min. In order to show clearly the peak splitting, we present in Fig. 1(b) a TOF spectrum at  $\theta_i = 34^\circ$  with improved signal-to-noise ratio. It is produced by adding seven "half-hour" measurements from different days; the result also emphasizes the reproducibility of the experiment. All TOF spectra between  $35^\circ$  and  $31^\circ$  have been reproduced several times, for different beam energies on the annihilation as well as on the creation branch, always showing the same splitting behavior. Near the zone boundary the phonon peak sharpens again, and only one dominant energy loss of  $\sim 11$  meV is observed. Besides these intense features, some small but sharp phonon losses are detected (shown as  $\times$ 's in Fig. 3). These peaks are only sharp at low surface temperatures and manifest themselves at higher temperatures as a broad buckled tail. We attribute these losses to bulk-state resonances arising from the large density of bulk states in that region.<sup>12</sup> In Fig. 2 a measured TOF spectrum of the annihilation branch at  $\theta_i = 62.5^\circ$  taken with a 18-meV beam is presented. Besides the energy gain at 11 meV a second unusually broad phonon peak at 15.7 meV, with  $Q = 1.49 \text{ \AA}^{-1}$ , is present. This mode is only detected close to the  $\bar{K}$  point and at higher surface temperatures.

Figure 3 shows a reduced-zone plot of the experimental and the theoretical surface phonon dispersion along the  $\bar{\Gamma}$ - $\bar{M}$  and  $\bar{\Gamma}$ - $\bar{K}$  directions. The theoretical dispersion curves are obtained by assuming a lattice-dynamical model Hamiltonian where the potential energy term is based on nearest-neighbor interactions and central forces. We have deliberately chosen a simple model so as to be free from too many unknown parameters and also to be able to obtain exact results using a quasianalytic technique. The technique is based on solving the equations of motion for Fourier-

transformed Green's functions which are defined in terms of the eigenmodes of the system.<sup>5</sup> The hierarchy of equations that emerge are handled by invoking an exponential ansatz for the displacement of atoms in the bulk crystal which then allows one to naturally match the bulk solutions onto the equations for the surface layer atoms. In the case of the Pt(111) surface this leads to nine coupled equations for the solutions along the  $\bar{\Gamma}$ - $\bar{K}$  direction, while the inherent symmetry along the  $\bar{\Gamma}$ - $\bar{M}$  direction yields only six such equations. In either case one is able to vary the interlayer and intralayer coupling constants for the first two layers and ob-

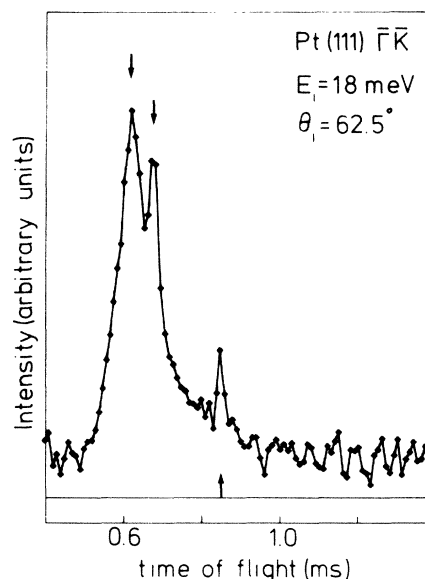


FIG. 2. TOF spectrum for the  $\bar{\Gamma}$ - $\bar{K}$  azimuth at a crystal temperature of 350 K and a He-beam energy of 18 meV at  $\theta_i = 62.5^\circ$ .

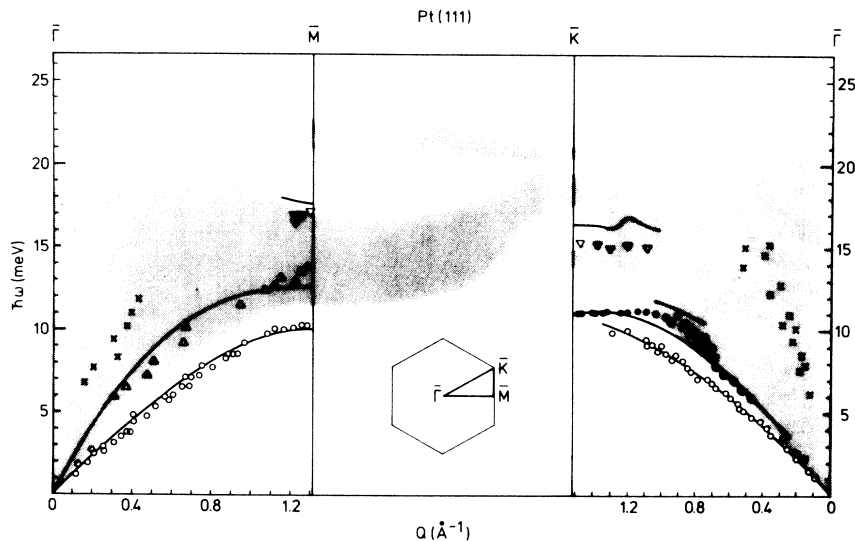


FIG. 3. Measured and calculated dispersion curves for Pt(111) (see text). Only theoretical dispersion curves with a vertical component are shown.

tain exact solutions for the surface modes using standard techniques. The phonon spectral densities that follow directly<sup>5</sup> from the calculated Green's functions for the atomic displacements are then plotted as a function of the phonon frequency for a given value of  $Q$ , the wave-vector component parallel to the surface. This method has the advantage of giving exact and analytical results with the choice of only one force constant to describe the bulk phonons. In the case of Pt a single-force-constant model does not give a perfect fit to the bulk phonon dispersion data; however, a two-force-constant model gives an even worse fit,<sup>13</sup> and the inclusion of a larger number of neighbors introduces too many free parameters. We have, therefore, found it reasonable to use the single force-constant model.

Let us first compare more specifically the phonon spectral densities calculated at the  $\bar{M}$  point (Fig. 4) and at the  $\bar{K}$  point (bottom right Fig. 5) with the corresponding experimental results in Fig. 3. The calculated densities exhibit in both cases three strong features located in the ranges 10–11 meV, 12–13 meV, and 16–18 meV. At the  $\bar{M}$  point each of the three features are mixed sagittal modes (vertical and longitudinal), while at the  $\bar{K}$  point none of them is mixed. As seen in Fig. 3, all features except the 12-meV pure longitudinal first-layer mode at the  $\bar{K}$  point are observed in experiment. This shows that pure longitudinal modes are not detected by He scattering under the present experimental conditions. On the other hand, it is very interesting that the  $\sim 16$ -meV mode is seen at the  $\bar{K}$  point. This mode is polarized longitudinally to the surface in the first layer and vertically with a larger amplitude in the second layer. Note, in summary, that while at the  $\bar{M}$  point both low-energy modes are seen in the experiment, at the  $\bar{K}$  point only one low-energy mode is detected. Only after moving away from  $\bar{K}$  towards the zone center does a lower branch with mixed polarization emerge.

An intriguing aspect in the surface phonon dispersion in Fig. 3 is the apparent splitting of the Rayleigh wave along the  $\bar{\Gamma}$ - $\bar{K}$  direction, commencing halfway down to the zone boundary. Such a splitting could only be reproduced in the calculated phonon spectral densities by substantial softening

of the intralayer force constant for the atoms in the first layer  $k_{11}=0.4k$ , where  $k$  is the force constant for the bulk atoms. The same behavior was recently inferred from the lattice-dynamical calculations of Bortolani<sup>12,14</sup> for the (111) surfaces of the noble metals (Cu, Ag, and Au). However, the experimental evidence presented so far is scarce.<sup>3,4,14</sup> To illustrate this point further, we present in Fig. 5 a series of spectral densities calculated for various values of  $Q$  along the  $\bar{\Gamma}$ - $\bar{K}$  direction. As just emphasized, this splitting does not appear at the  $\bar{K}$  point, but rather as one moves away from it towards  $\bar{\Gamma}$ . In fact, it is already very pronounced at  $Q=1.28 \text{ \AA}^{-1}$  as a "peel-off" branch from the strong 11-meV feature at the  $\bar{K}$  point. The intensity of this lower-energy branch grows as one moves towards the zone center

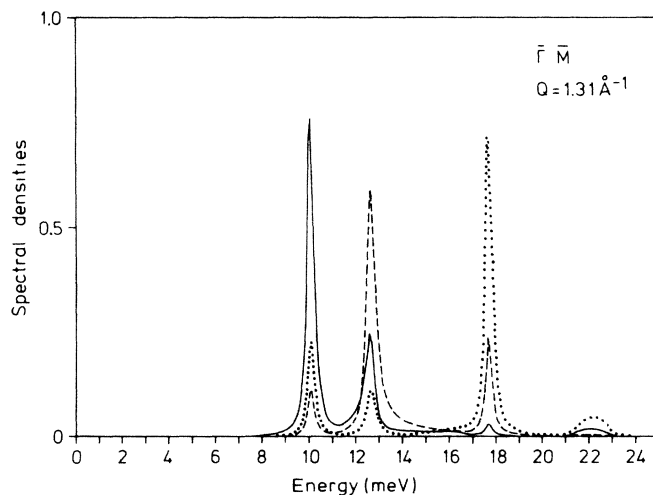


FIG. 4. Phonon spectral density of Pt(111) at the  $\bar{M}$  point. The full and dotted lines represent the vertical motion of the first and second layer atoms in the sagittal plane, respectively. The dashed line represents the longitudinal motion of the first-layer atoms in the sagittal plane. The force constants used are  $k_{11}=0.4k$ ,  $k_{12}=1.1k$  where  $k$ , the bulk force constant, is  $4.83 \times 10^4$  dyne/cm.

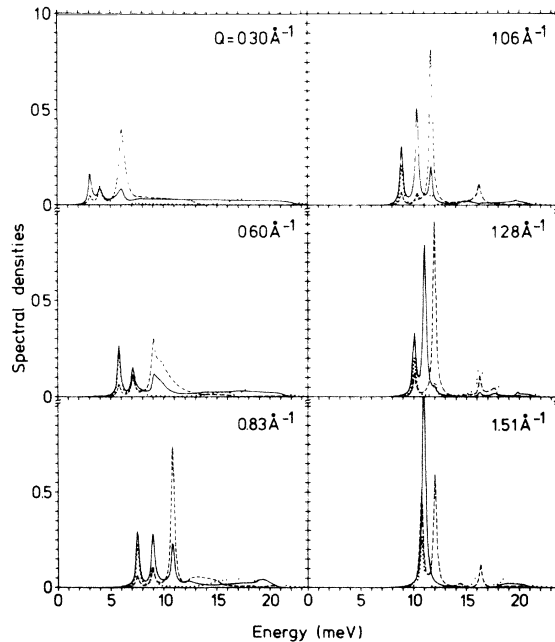


FIG. 5. Phonon spectral density series of Pt(111) along the  $\bar{\Gamma}$ - $\bar{K}$  azimuth with  $Q$  as a parameter. The notation and constants are the same as in Fig. 4 ( $Q = 1.51 \text{ \AA}^{-1}$  at the  $\bar{K}$  point).

and eventually becomes the dominant mode, in accordance with our experimental findings. Actually, this mode is the Rayleigh wave which is polarized shear-horizontally at large  $Q$  values and thus is not detectable under the present conditions. The high-energy branch which dominates at large  $Q$  values seems to be the so-called pseudo-Rayleigh-wave.<sup>12,14,15</sup> Another interesting feature in the spectral density plots is the appearance of yet another branch with vertical polarization and localization of amplitude in the first layer around  $Q = 1.06 \text{ \AA}^{-1}$ . This resonance mode, however, exists only for a short interval before merging in the bulk band. Indeed, a buckling of the experimental dispersion curve is observed in this  $Q$  range, probably because of

the presence of this resonance mode. Last, but not least, the second-layer perpendicular mode emerges as a strong contender in the spectral density plots at and near the  $\bar{K}$  point (and similarly at and near the  $\bar{M}$  point), probably being seen in the TOF spectra taken at higher surface temperatures. The complex splitting behavior that the calculations display along the  $\bar{\Gamma}$ - $\bar{K}$  direction is not found along the  $\bar{\Gamma}$ - $\bar{M}$  direction, probably as a result of the higher symmetry along the latter. In the  $\bar{\Gamma}$ - $\bar{M}$  direction there are two modes over the whole Brillouin zone which are polarized vertically with maximum amplitudes in the first Pt layer. The low-energy branch is the vertically polarized Rayleigh wave, whereas the high-energy branch is a mixed sagittal mode. Over the whole Brillouin zone in the  $\bar{\Gamma}$ - $\bar{M}$  direction, the Rayleigh wave is the dominant feature, in agreement with the experimental findings.

In summary, the agreement between the experimental and theoretical dispersion curves, shown in Fig. 3, is quite good considering the use of such a simple model based only on nearest-neighbor interactions. Most of the salient features of the observed dispersion curves can be reproduced provided one assumes a substantial softening of the intralayer force constant. An effect of similar magnitude ( $k_{11} = 0.48k$ ) was also present in the calculations of Bortolani and co-workers,<sup>12,15</sup> when they tried to obtain a fit to the dispersion of surface phonons on Ag(111). A convincing physical explanation is still missing. On the other hand, electron-energy-loss measurements on Ni(100) (Ref. 16) and Cu(100) (Ref. 17) indicate no softening of the  $k_{11}$  force constant. In order to fit the experimental dispersion curves of these surfaces, it was sufficient to stiffen the interlayer force constant  $k_{12}$  by 20%. This suggests that the difference in the interatomic force field at the surface may originate in the different structure of the two types of surfaces [(111) vs (100)].

*Note added.* After this paper was submitted for publication, we became aware of a recent publication<sup>18</sup> on the same system.

Enlightening discussions with Vittorio Celli and Harald Ibach as well as the skillful technical help of Karl Veltmann are gratefully acknowledged.

<sup>1</sup>J. P. Toennies, *J. Vac. Sci. Technol. A* **2**, 1055 (1984).

<sup>2</sup>H. Ibach and T. S. Rahman, in *5th International Conference on Solid Surfaces*, edited by R. Vanselow and R. Howe, Springer Series in Chemical Physics, Vol. 35 (Springer, Berlin, 1985), p. 455.

<sup>3</sup>R. B. Doak, U. Harten, and J. P. Toennies, *Phys. Rev. Lett.* **51**, 578 (1983); M. Cates and D. R. Miller, *Phys. Rev. B* **28**, 3615 (1983).

<sup>4</sup>U. Harten, J. P. Toennies, and Ch. Wöll, *Faraday Discuss. Chem. Soc.* (to be published).

<sup>5</sup>T. S. Rahman, J. E. Black, and D. L. Mills, *Phys. Rev. B* **25**, 883 (1982); J. E. Black, T. S. Rahman, and D. L. Mills, *ibid.* **27**, 4072 (1983).

<sup>6</sup>K. Kern, R. David, and G. Comsa, *Rev. Sci. Instrum.* **56**, 369 (1985).

<sup>7</sup>A detailed description of the apparatus will be given elsewhere.

<sup>8</sup>G. Comsa, R. David, and B. J. Schumacher, *Rev. Sci. Instrum.* **52**, 789 (1981).

<sup>9</sup>B. Poelsema, R. L. Palmer, G. Mechttersheimer, and G. Comsa, *Surf. Sci.* **117**, 60 (1982).

<sup>10</sup>K. Kern, R. David, R. L. Palmer, and G. Comsa, *Phys. Rev. Lett.* **56**, 620 (1986).

<sup>11</sup>K. Kern, R. David, and G. Comsa, *Surf. Sci.* **164**, L831 (1985).

<sup>12</sup>V. Bortolani, A. Franchini, and G. Santoro, in *Dynamical Phenomena at Surfaces, Interfaces and Superlattices*, edited by F. Nizzoli, K. H. Rieder, and R. F. Willis, Springer Series in Surface Science, Vol. 3 (Springer, Berlin, 1985), p. 92.

<sup>13</sup>J. E. Black, F. C. Shanes, and R. F. Wallis, *Surf. Sci.* **133**, 199 (1983).

<sup>14</sup>V. Bortolani, G. Santoro, U. Harten, and J. P. Toennies, *Surf. Sci.* **148**, 82 (1984).

<sup>15</sup>G. W. Farnell, in *Physical Acoustics*, edited by W. P. Mason and R. N. Thurston (Academic, New York, 1970), Vol. VI, p. 109.

<sup>16</sup>M. Rocca, S. Lehwald, and H. Ibach, *Surf. Sci.* **138**, L123 (1984).

<sup>17</sup>M. Wuttig, R. Franchy, and H. Ibach, *Solid State Commun.* **57**, 445 (1986).

<sup>18</sup>U. Harten, C. Wöll, and J. P. Toennies, *Phys. Rev. Lett.* **55**, 2308 (1985).

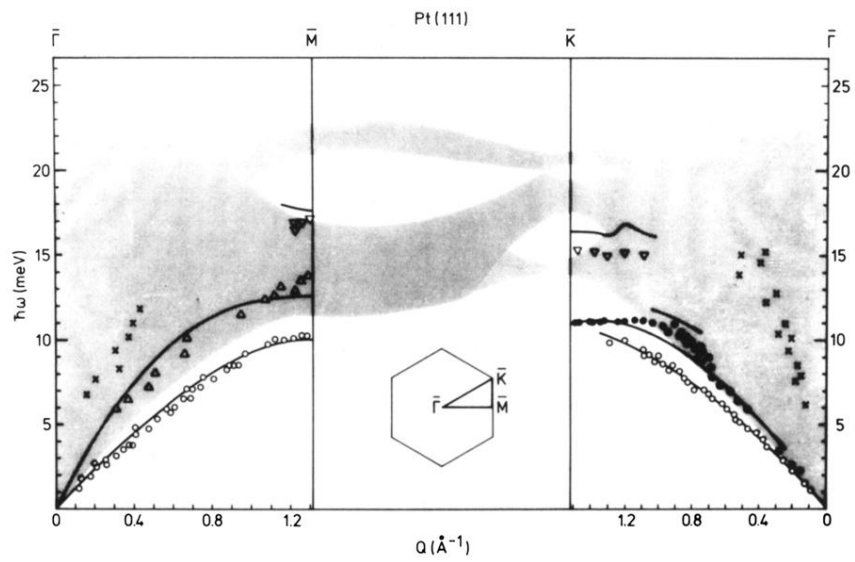


FIG. 3. Measured and calculated dispersion curves for Pt(111) (see text). Only theoretical dispersion curves with a vertical component are shown.